



A novel hybrid model for lung and colon cancer detection using pre-trained deep learning and KELM

Gowthamy J.^{*}, Subashka Ramesh

Department of Computer Science and Engineering, SRM Institute of Science and Technology, Ramapuram, Chennai, India



ARTICLE INFO

Keywords:

CNN
KELM
MB-DMOA
ResNet-50
InceptionV3
LC cancer
DenseNet
GlaS
Histopathological images

ABSTRACT

Cancer poses a significant threat to life due to its aggressive nature, high potential for metastasis, and heterogeneity. Globally, both men and women are mostly affected by lung and colon (LC) cancer. Early and accurate detection is essential to enhance the well-being of patients facing LC cancer. The traditional techniques face challenges such as low accuracy and high execution time. This work combines the pre-trained deep learning (DL) models like ResNet-50, InceptionV3, and DenseNet with Kernel Extreme Learning Machine (KELM) for the accurate and fast diagnosis of LC cancer using histopathology images. The pre-trained DL models provide a strong foundation for feature extraction, capturing intricate patterns indicative of cancerous tissues. Feature fusion combines the complementary strengths of multiple pre-trained models, enhancing the method's ability to capture diverse features and improve classification accuracy. KELM efficiently handles the high-dimensional feature space generated by the DL models, ensuring fast and accurate classification. Mutation Boosted Dwarf Mongoose Optimization Algorithm (MB-DMOA) further optimizes the model parameters, mitigating the risk of getting stuck in local optima and facilitating better convergence towards the global optimum. By leveraging the advantages of each technique and integrating them into a cohesive framework, the proposed approach achieves superior performance in diagnosing LC cancer, ultimately improving patient outcomes. The proposed study attains accuracy (98.9%), F1-score (97.6%), specificity (96.5%), precision (96.7%) and sensitivity (95.8%). The results illuminate the efficacy of this approach within therapeutic environments.

1. Introduction

Lung and colon (LC) cancer stands as prominent contributors to global cancer-related fatalities, underscoring cancer's status as a significant and pressing health concern worldwide (Tummala et al., 2023). Aging, cigarette smoking, and genetics are important risk factors for both types of cancer, which can have a terrible impact on patients as well as their families. Enhancing patient outcomes, strengthening treatment plans, and ultimately reducing mortality rates all depend on the prompt identification and precise diagnosis of these cancers. The introduction of modern medical imaging techniques and computational technology has created new frontiers for improving cancer diagnosis (Rajesh et al., 2020). In particular, the fusion of DL with optimization algorithms presents a promising avenue for more accurate, efficient, and reliable cancer diagnosis.

Unchecked cell growth occurs in lung tissues, which is a common and serious feature of lung cancer. Two possible manifestations are squamous cell carcinoma and adenocarcinoma. In accordance to the World

Health Organization (WHO), lung cancer is the most prevalent cause of cancer-related death globally, accounting for 1.76 million deaths annually. Primarily impacting the colon and rectum, colorectal cancer is an alternate term for colon cancer. Adenocarcinoma stands out as the most common subtype of colon cancer. Ranked as the third most diagnosed disease globally, colorectal cancer resulted in approximately 935,000 fatalities in 2020 (Alboaneen et al., 2023). When LC cancer is detected early, treatment outcomes improve dramatically (Elnakib et al., 2020). Regular screening and timely intervention often lead to less invasive treatment options and better outcomes for patients.

Tissue sample histopathological analysis is a common technique for cancer diagnosis (Li et al., 2021). To determine whether cancer cells are present in the tissue, a microscope examination is required. However, this process consumes considerable time, labor, and specialized expertise (Ho et al., 2022). Additionally, it is prone to inter-observer variability, signifying that different pathologists may interpret the same image differently. One of the primary challenges in histopathological image analysis is the complexity of cancer tissues. Cancerous tissues

* Corresponding author.

E-mail addresses: gowthamyjsrm@gmail.com (J. Gowthamy), subashka@gmail.com (S. Ramesh).

exhibit significant heterogeneity, and distinguishing between benign and malignant cells, especially at an early stage, a challenging even for experienced pathologists. Furthermore, the volume of histopathological data generated in clinical practice has grown exponentially, increasing the need for more efficient and accurate diagnostic methods.

Convolutional neural network (CNN) is the most widely used deep learning(DL) method for analyzing medical images (Baranwal et al., 2021). Across various tasks like segmentation, object detection, and image classification, DL models exhibit exceptional performance. They prevent the requirement for human feature engineering and specialized knowledge by autonomously extracting features from the data and generating predictions based on these characteristics. Nonetheless, achieving success with DL models in medical image analysis necessitates proper parameterization and training, both of which pose challenges. Several modified CNN models have been generated in recent years. The most common patterns are the input layer, convolutional layer, and classification layer. Through neurons, the input data is transformed. Each neurons are connected to the previous convolutional layer. The GoogleNet and the AlexNet are the DL models with the same neural type. These models provide superior efficiency but are time-consuming. Training DL models heavily depend on optimization algorithms including Ant Colony Optimization (ACO) and Particle Swarm Optimization (PSO), as outlined by Raihan and Nahid (2023) and Ye et al. (2023). The aforementioned techniques intend to minimize the difference between the model's predictions and the actual outcomes by altering the model's parameters. Traditional optimization techniques, such as Stochastic Gradient Descent (SGD) (Naseer et al., 2022), have been widely employed in DL. However, these algorithms sometimes lead to insignificant results. Subsequently, the co-evolutionary optimization algorithm utilizes prior knowledge of sparse optimal solutions to guide solution generation by clustering and dividing the population. It efficiently calculates optimal sparsity and directs offspring generation accordingly, enhancing solution quality (Zhang et al., 2024). However, the algorithm's effectiveness heavily depends on the availability and accuracy of this prior knowledge, posing limitations. Further, the Pearson correlation-based adaptive variable grouping method is employed to gauge similarities in the evolutionary trends of variables. Through the utilization of Pearson correlation coefficients, it effectively partitions variables, thereby establishing the foundation for a weighted optimization framework (Zhang et al., 2023). However, the method's effectiveness is tempered by the complexities inherent in larger-scale optimization problems.

The challenges faced by the traditional approaches are high time consumption and low accuracy. To tackle this challenge, pre-trained models such as ResNet, DenseNet, and Inception V3 are utilized. The advantages of these three models are combined into a single vector that improves the model to detect intricate patterns efficiently. KELM is used to classify high-dimensional data with stable performance. The integration of the mutation technique with the DMOA provides enhanced adaptability, exploitation, and exploration. Overall, the approach provides more efficient classification. (Akinola et al., 2022).

1.1. Research objectives

Utilizing DL and optimization approaches, this study endeavors to leverage histopathology images for precise and timely diagnoses of LC cancer. The model seeks to achieve the following primary research objective.

- Developing and enhancing hybrid DL models for the classification of malignant and non-cancerous tissue regions in histopathology images is the aim of this research. These models will integrate pre-trained DL architectures with the Kernel Extreme Learning Machine (KELM).
- To investigate the role of advanced optimization techniques, including the Mutation Boosted Dwarf Mongoose Optimization

Algorithm (MB-DMOA), in fine-tuning the parameters of the KELM model for improved classification performance.

- Assessing the productiveness of the proposed models involves applying rigorous quantitative metrics, across a range of datasets. These include the Gland Segmentation in Colon Histology Images (GlaS) dataset and the LC Cancer Histopathological Image (LC25000) dataset. To explore the potential clinical applications and implications of these advanced computational methods in aiding pathologists and clinicians in early cancer detection and diagnosis.

1.2. Contributions

This study makes significant contributions to the fields of machine learning (ML) and cancer diagnostics in various aspects:

Integration of Pre-trained DL Models with KELM: While both DL and KELM have been individually used in various applications, their combination in the context of medical image analysis, particularly for cancer diagnosis, is relatively novel. This integration allows for the efficient handling of high-dimensional image data and the exploitation of both learned features and extracted representations from pre-trained models.

Feature Fusion for Enhanced Pattern Recognition: The feature fusion technique employed in the proposed methodology enhances the approach's capability to capture intricate patterns indicative of cancerous tissues by combining the representations learned by multiple pre-trained DL models. This synergistic fusion of features leads to improved diagnostic accuracy and robustness.

Optimization with MB-DMOA: The utilization of MB-DMOA addresses the local optima problem commonly encountered in optimization tasks, thereby enhancing the efficiency and effectiveness of the overall diagnostic system. The incorporation of this novel optimization algorithm adds a layer of adaptability and exploration to the model, contributing to its superior performance in histopathological image classification.

The arrangement of the article is as follows: Section 2 examines the literature, Section 3 details the proposed model for classifying LC cancer and the optimization strategy, Section 4 unveils the results and discussions from experiments on the LC25000 and GlaS datasets, and finally, Section 5 concludes the paper with reflections on potential directions for future research.

2. Literature review

An essential component of oncology is precision in cancer diagnosis, which directly influences treatment outcomes and patient care. This literature review is dedicated to examining existing research focusing on the utilization of DL in cancer diagnosis, incorporating KELM, pre-trained DL models, and optimization algorithms such as DMOA and MB-DMOA.

2.1. DL Applications in Cancer Diagnosis

Within the domain of ML, DL, a distinct category, has showcased notable achievements across diverse domains, with medical image analysis standing out prominently. The use of DL models, particularly CNNs, for the analysis of medical images has increased recently, aiming to diagnose cancer. The inherent ability of CNNs to autonomously acquire hierarchical features from raw data positions makes them apt for complex image analysis assignments.

To classify histopathological images associated with LC cancer, various inquiries have explored the utilization of DL. As an illustration, Mangal et al. (2020) constructed a CNN utilizing the LC25000 dataset to diagnose LC cancer in histopathology images. Despite the CNN model showing enhanced accuracy in diagnosing both LC conditions, its overall performance fell short of optimal. Hasan et al. (2022) illustrated a DCNN for automatic detection of colon cancer. The DCNN model offered better

detection accuracy. However, the model utilized a smaller dataset. Similarly, Yu et al. (2021) introduced a cancer diagnosis model particularly, for colorectal cancer known as semi-supervised DL, which accurately detected colorectal cancer and provided better performance. Nevertheless, the model had labeled data, which affected the productiveness. A CNN architecture designed specifically for recognizing lung cancer in histopathological images was created by Hatuwal and Thapa (2020). Although the CNN model showcased better accuracy in a short timeframe, it necessitated a larger dataset for effective training. In a parallel context, Sakr et al. (2022) presented a streamlined CNN model aimed at detecting colon cancer. Despite demonstrating robustness, enhanced accuracy, reduced processing time, and cost-effectiveness, the overall performance of the approach fell short of the expected levels. Taking a different approach, Jiao et al. (2021) devised a CNN strategy for classifying whole-slide images in colon cancer. While autonomously recognizing the tumor microenvironment in colorectal cancer, the stain normalization process yielded less-than-optimal outcomes. A deep neural network (DNN) developed by Lai et al. (2020) successfully predicted the presence of non-small cell lung cancer (NSCLC). The DNN approach combined both clinical and heterogeneous data and provided high prediction accuracy. However, the model utilized a less data sources. Lee et al. (2021) presented a screening method for the diagnosis of colorectal cancer known as the automated DL-based microsatellite instability (MSI) classifier, which is low-cost and time-effective. Yet, the difference between the prognostic significance of homogeneous and heterogeneous tumors was not identified. Zhou et al. (2021) demonstrated a weakly supervised DL model, which identified the cancerous tissues in whole slide images (WSIs) and offered a better performance with time effectiveness. However, the approach required more hand-crafted features. Salimy et al. (2023) designed a DL-based multi-omics and data integration tool to classify colon cancer. The model identified the high and low-risk groups and offered an improved mean square error (MSE) rate. Yet, the computing power of the model was low.

2.2. Utilization of Pre-trained DL Models

Within medical image analysis, the integration of transfer learning, a method leveraging pre-trained models from a source task to enhance performance in a target task, has surged. Employing pre-trained models like InceptionV3, DenseNet, and ResNet-50 as either task-specific initializations or feature extractors has gained prominence (Rajesh and Chandrasekar, 2023). Research has affirmed that the utilization of pre-trained models significantly elevates the efficacy of DL models in the domain of cancer diagnosis. Yahia Ibrahim and Talaat (2022) highlighted the identification of LC cancer using an EfficientNetB7 DL model paired with Double Contrast Limited Adaptive Histogram Equalisation (Double-CLAHE) and Discrete Wavelet Transform (DWT). While the model achieved improved detection accuracy, its overall efficacy was relatively diminished. To aid in the classification and identification of LC cancer, Tasnim et al. (2021) introduced a CNN model that incorporated MobileNetV2, max pooling, and average pooling layers uniquely. The model demonstrated commendable detection accuracy, yet its evaluation relied on a limited dataset. Attallah et al. (2022) developed a lightweight DL approach that combines principal component analysis (PCA), discrete wavelet transform (DWT), and fast Walsh-Hadamard transform (FHWT) to diagnose LC cancer. The outcomes of the model indicated its cost-effectiveness and efficacy. Nevertheless, the impact of the feature extraction process, generating a substantial number of new features through PCA and FHWT, posed a challenge to the model's performance. On a separate front, Hadiyoso et al. (2023) classified images of LC histological cancer using the CLAHE approach and a CNN model with a VGG16 architecture. While the model exhibited higher accuracy and utilized a larger dataset at a lower cost, its overall output remained below expectations.

2.3. KELM and optimization algorithm

KELM, a feedforward neural network distinguished by a lone hidden layer employs kernel functions to address nonlinear challenges, marking a significant advantage over conventional ELM.

The benefits of KELM include faster training times, better generalization performance, and the ability to handle large-scale data. Demonstrating effectiveness in various domains, KELM has successfully found applications, particularly in tasks like the classification of medical images.

To attain optimal performance in ML models, meticulous fine-tuning of parameters is essential, a task streamlined by the deployment of optimization algorithms. A groundbreaking addition to this field is Dwarf Mongoose Optimization (DMOA), an approach inspired by the foraging behaviors of dwarf mongooses, as clarified by Hadiyoso et al. (2023) and Agushaka et al. (2022). DMOA is characterized by its simplicity, ease of implementation, and ability to escape local optima. MB-DMOA is an enhanced version of DMOA that incorporates mutation operators to boost its exploration and exploitation capabilities. MB-DMOA has shown promising results in optimizing various engineering problems.

While the application of DMOA and MB-DMOA in medical image analysis has not been extensively explored in the literature, their achievements in diverse domains suggest potential benefits for fine-tuning ML model parameters in cancer diagnosis. Obayya et al. (2023) published the first study on the usage of a Tuna Swarm Algorithm with DL (TSADL) to detect LC cancer in biomedical photos in 2023. The TSADL model achieved higher precision; however, the overall performance of the approach was subpar.

2.4. Integration of DL and KELM

An emerging study that combines the best features of both methodologies is the fusion of KELM with DL. DL models learn hierarchical features from raw data, while KELM provides fast training times and good generalization performance. The fusion of DL models and KELM offers researchers an avenue to enhance the classification performance of histopathological images, capitalizing on the synergies between these techniques for more effective outcomes in cancer diagnostics.

Since this topic is still in its early stages, more research is required to properly understand the advantages and restrictions of integrating KELM and DL in the context of cancer identification. The examination of the literature underscores the significant advancements achieved in cancer diagnosis by leveraging DL applications and optimization techniques. Notably, pre-trained DL models hold promise for enhancing the efficiency of tasks related to cancer classification. KELM offers fast training times and good generalization performance, making it a promising candidate for medical image analysis. The combination of DL and KELM with advanced algorithms, like MB-DMOA, for optimizing model parameters presents a viable approach to enhance the accuracy and efficacy of cancer identification using histopathology images. A more detailed explanation of choosing pre-trained DL models such as ResNet-50, InceptionV3, and DenseNet for the proposed strategy is as follows:

Superior Performance: ResNet-50, InceptionV3, and DenseNet are widely recognized and extensively evaluated DL architectures that have demonstrated state-of-the-art performance on various image classification tasks, including medical image analysis. Their effectiveness in learning discriminative features from images makes them suitable candidates for our application in diagnosing LC cancer from histopathology images.

Availability and Accessibility: These pre-trained models are readily available and accessible through popular DL frameworks such as TensorFlow and PyTorch. Their implementations are well-documented, and pre-trained weights are often provided, allowing for easy integration and utilization in our study without the need for extensive model

training from scratch.

Versatility and Flexibility: ResNet-50, InceptionV3, and DenseNet are versatile architectures that have been successfully applied to a wide range of image analysis tasks beyond image classification, including object detection, segmentation, and feature extraction. Their flexibility allows for adaptation to different domains and datasets, making them suitable for our specific application in diagnosing cancer from histopathology images.

While there are certainly other DL architectures and methods available, we chose ResNet-50, InceptionV3, and DenseNet for their established performance, accessibility, and suitability to our research objectives. Additionally, the extensive literature and community support surrounding these models provide a solid foundation for our study and facilitate comparison with existing works in the field.

3. Methodology

The proposed study's design is illustrated in Fig. 1. The success of a DL-based cancer diagnosis model depends on robust datasets, such as LC25000 and GlaS datasets, and meticulous preprocessing steps. This involves resizing images, normalization, and partitioning for effective training and evaluation. The model's generalization is enhanced, and the overfitting problem is prevented using the data augmentation process. This includes random rotation, elastic deformation, flipping, and zoom factor. The hybrid model combines the strengths of pre-trained DL models such as ResNet-50, InceptionV3, and DenseNet with the KELM for accurate cancer diagnosis. Feature extraction employs DL models, including ResNet-50, InceptionV3, and DenseNet, to capture high-level features, followed by fusion to enhance pattern recognition. This

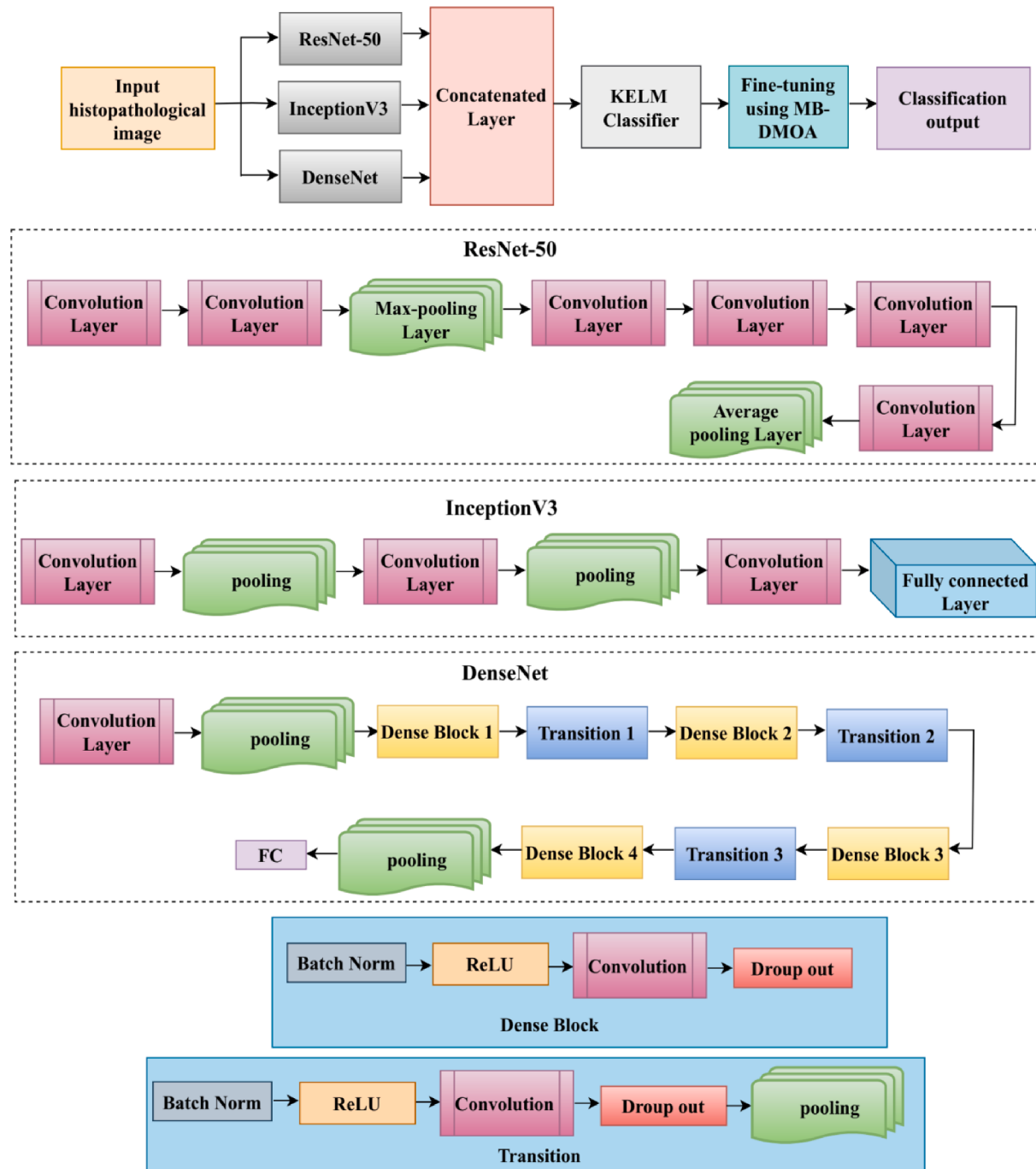


Fig. 1. Proposed approach's general framework.

feature fusion combines features from the three pre-trained models into a single comprehensive feature. The final phase involves KELM, acting as the classification engine, efficiently handling high-dimensional data. The final predictions for the diagnosis of LC cancer are obtained as the output of the KELM classifier. An accurate and robust solution for histopathological image-based cancer diagnosis is achieved by integrating feature extraction with pre-trained models and classification with KELM. The training strategy encompasses fine-tuning DL models and training KELM, utilizing regularization techniques like dropout and batch normalization. The optimization phase involves MB-DMOA, a sophisticated algorithm inspired by dwarf mongoose behavior, to refine KELM hyperparameters. This approach ensures enhanced exploration, efficient exploitation, and adaptability, contributing to superior model performance.

3.1. Data Collection

High-quality and well-structured datasets are the foundation of the successful DL-based cancer diagnosis model. In this section, the process of gathering the histopathological image datasets, which include the LC25000 dataset and GlaS dataset is discussed. Additionally, data preprocessing is employed for evaluation.

LC25000 Dataset: The LC25000 dataset serves as a valuable resource for the proposed study. This dataset, as outlined by Borkowski et al. (2019) and accessible at (<https://www.kaggle.com/datasets/andrewmvd/lung-and-colon-cancer-histopathological-images/data>), comprises histopathological images of LC tissues categorized into five classes: lung adenocarcinoma (lung_aca), lung benign tissue (lung_n), colon adenocarcinoma (colon_aca), lung squamous cell carcinoma (lung_scc), and colon benign tissue (colon_n). Drawing from various sources, including research facilities and clinical settings, the dataset offers a comprehensive and diverse representation of LC cancer tissues.

GlaS Dataset: The GlaS dataset is specifically designed with gland segmentation in colon histology images as its primary objective. It consists of benign and malignant colon tissue samples, which are further divided into glandular Regions (<https://www.kaggle.com/datasets/sani84/glassiccai2015-gland-segmentation>). This dataset holds significant research value, given that precise gland segmentation plays a pivotal role in diagnosing colon cancer and comprehending the extent of tissue involvement.

3.2. Data preprocessing and augmentation

To ensure that the gathered datasets are suitable for training the proposed model, data preprocessing and augmentation steps are applied.

Image resizing: In the image resizing step, the histopathological images are resized to a 224x224 dimension to ensure uniformity and reduce computational complexity.

Image normalization: In the normalization step, the pixel values are normalized to enhance the proposed model's convergence during training. A mean subtraction and standard deviation scaling are applied to bring pixel values to a standard range [-1, 1].

Data splitting: The dataset is split into testing, validation, and training sets during the data partitioning phase. Testing uses 20 % of the data, validation uses 10 %, and training uses 70 % of the data on average. In label encoding, the class labels are encoded as numerical values to facilitate model training.

Data augmentation: In data augmentation, overfitting is mitigated and model generalization is improved. The process of creating enhanced versions of the original images involves applying adjustments such as rotation, random cropping, and horizontally and vertically flipping images. At random, the images are flipped based on three different axes. Random rotation technique rotates the image randomly within the range $0^\circ, 15^\circ, 30^\circ, 60^\circ$ or 90° . Zooming involves scaling the images randomly

with a range of $\pm 10\%$ or $\pm 20\%$. The elastic deformation is performed for the values 2,5,8 or 10 voxels based on a square deformation grid. Augmentation enhances the model's ability to recognize more robust features by introducing diversity to the training dataset.

3.3. Feature Extraction and Fusion using Hybrid Pre-trained DL Models

The first component of the proposed hybrid model involves leveraging DL models, specifically ResNet-50, InceptionV3, and DenseNet to extract high-level features from histopathological images. These pre-trained models have already learned intricate features from diverse images, and the proposed model aims to capitalize on their knowledge. The feature extraction process is mathematically represented as follows:

$$F_R = \text{ResNet-50}(I) \quad (1)$$

$$F_I = \text{InceptionV3}(I) \quad (2)$$

$$F_D = \text{DenseNet}(I) \quad (3)$$

where I represent an input histopathological image, F_R , F_I and F_D denotes the extracted features from ResNet-50, InceptionV3, and DenseNet respectively.

These operations yield feature vectors F_R , F_I F_D that capture the salient characteristics of the input image I as learned by the respective pre-trained models.

The next critical step is feature fusion, which involves combining features from pre-trained models into a single comprehensive feature vector. This process significantly enriches the feature representation and enhances the model's ability to discern subtle patterns indicative of cancerous tissues. Mathematically, feature fusion is expressed as follows:

$$F = [F_R, F_I, F_D] \quad (4)$$

where F represents the fused feature vector and $[F_R, F_I, F_D]$ denotes the concatenation of the feature vector F_R , F_I and F_D extracted by ResNet-50, InceptionV3, and DenseNet respectively.

3.3.1. Fine-tuning Pre-trained Models

One popular transfer learning technique is fine-tuning, involving taking a pre-trained model initially learned on a large dataset and then training it on a smaller dataset customized for the specific goals of the proposed practice. The histopathology image datasets are utilized for fine-tuning the pre-trained models (ResNet-50, InceptionV3, and DenseNet) in the proposed strategy.

The weights of the pre-trained model are adjusted during the fine-tuning phase to minimize the loss function, measuring the discrepancy between the model's predictions and the actual labels. The proposed model utilizes the categorical cross-entropy loss function for its classification tasks. Formally, the cross-entropy loss function is defined as follows:

$$L(y, p) = - \sum (y_i * \log(p_i)) \quad (5)$$

where $L(y, p)$ is the loss for a given sample, y is the actual label (one-hot encoded), p is the probability distribution prediction from the softmax layer, and i iterates over the number of classes.

Iteratively adjusting the model's weights to minimize the loss function is achieved by using an optimization algorithm, usually SGD or its derivatives like Adam. The learning rate hyperparameter determines the optimization process's step size.

3.4. Classification with KELM

The final component of the proposed hybrid model involves the KELM, which serves as the classification engine. KELM is particularly

well-suited for this task due to its ability to efficiently classify data in high-dimensional spaces, which is often necessary when dealing with complex image features. The classification procedure is outlined in the following manner:

$$f(X) = \sum_{i=1}^N \alpha_i K(X, X_i) + b \quad (6)$$

where K denote the kernel function, X represent the fused feature vector F , $f(X)$ represent the decision function, which assigns an input feature vector X to a specific class, α_i is the KELM's output layer weights, X_i represents the support vectors from the training data, and b is the bias.

The kernel function $K(X, X_i)$ calculates the similarity between the input feature vectors X and the support vectors X_i . The different kernel function (e.g., linear, polynomial, RBF) is employed based on the problem's characteristics. The specific choice of the kernel function is part of the model configuration.

The final prediction for the recognition of LC cancer is made by the constructed hybrid model using the outcomes of the KELM classifier. The overarching objective is to maximize classification accuracy by optimizing the parameters of both the KELM classifier and the DL models (ResNet-50, InceptionV3, and DenseNet). By integrating feature extraction with DL models and classification with KELM, the proposed model aims to provide a robust and accurate solution for histopathological image-based cancer diagnosis.

3.4.1. Training KELM Classifier

A comprehensive feature representation is generated by concatenating the feature vectors extracted from the pre-trained models. This resulting concatenated feature vector becomes the input for training the KELM classifier.

KELM is an extension approach for the ELM that adds a kernel function to supervised learning. This function simplifies non-linear classification by mapping the input data into a higher-dimensional space.

The training process of KELM involves finding the weight matrix's output (β) that minimizes the objective function, defined as:

$$J(\beta) = \|H\beta - T\|^2 + \lambda \|\beta\|^2 \quad (7)$$

where $J(\beta)$ is the objective function, H is the output matrix of hidden layer, β is the weight matrix's output, T is the target matrix (one-hot encoded labels), and λ is the regularization parameter, which prevents overfitting by penalizing large weights.

The solution β is obtained using:

$$\beta = H^+ T \quad (8)$$

where H^+ is the Moore-Penrose generalized inverse of matrix H .

Training ensures the incorporation of hierarchical features from the DL models and classification boundaries from KELM. This process involves both training the KELM classifier and fine-tuning pre-trained models. This synergy ensures the hybrid model's efficacy in diagnosing cancer accurately from histopathological images.

Regularization Techniques: Regularization methods like batch normalization and dropout are used to avoid overfitting. The model's capacity to generalize to new data is improved by these techniques.

3.5. MB-DMOA

MB-DMOA, an enhancement of the DMOA, drew inspiration from the compensatory behavioral adaptation of dwarf mongooses (Agushaka et al., 2022). It incorporates the polynomial mutation operator to improve the original DMOA's exploration and exploitation capabilities. The MB-DMOA is provided in Algorithm 1. The algorithm consists of three main phases: Alpha group, Scout group, and Optimization procedures. MB-DMOA enhances the performance of KELM by

effectively tuning its hyperparameters. The process involves the following steps:

Algorithm 1: Pseudocode of the MB-DMOA

```

Define hyperparameters such as Objective Function (Fitness Function), Number of
Variables, Variable Bounds, Population Size, Maximum Iterations and Distribution
Index ( $\eta$ )
Define search space for each hyperparameter
Initialize the population randomly within variable bounds
Calculate the fitness function using Equation (16)
Select alpha female ( $\alpha$ ) based on fitness probabilities using Equation (9)
while( $T < M_T$ )
for( $i = 1$  to  $N$ )
    Update candidate food position using Equation (10)
    Update sleeping mode using Equation (11)
    Compute average sleeping mound value( $\varphi$ ) using Equation (12)
    Update the position of the scout mongoose based on  $\varphi$  value using Equation (13)
    for(each solution in the population)
        Compute mutation factor( $\delta$ ) using polynomial distribution using Equation (14)
        Generate a new solution using Equation (15)
    end for
    Update alpha female ( $\alpha$ ) based on new fitness probabilities
end for
 $T = T + 1$ 
end while
Return optimal solution
Stop

```

3.5.1. Population Initialization

The first step in MB-DMOA is the potential solution's population initialization. For the KELM model, each solution represents a distinct set of hyperparameter values.

In the alpha group, the alpha female (α) is selected based on a probability value calculated as follows:

$$\alpha = \frac{f_t}{\sum_{i=1}^n f_i} \quad (9)$$

where f_i represents the fitness of each solution in the population

Every mongoose sleeps in the original sleeping mount, with the value set to '0'. The algorithm utilizes the following equation to determine the candidate's food position:

$X_{i+1} = X_i + \varphi \cdot peep(10)$ where X_{i+1} is the new candidate's food position, φ is a random number that is uniformly distributed between [-1,1], and $peep$ represents the alpha female's vocalization.

The sleeping mound is adjusted using the provided equation after each iteration:

$$sm_i = \frac{f_{t+1} - f_t}{\max\{|f_{t+1}|, |f_t|\}} \quad (11)$$

The following formula is used to calculate the average value of the sleeping mound:

$$\varphi = \frac{\sum_{i=1}^n sm_i}{n} \quad (12)$$

When the babysitting exchange requirement is met, the algorithm proceeds to the scouting stage.

3.5.2. Exploration and Exploitation

The algorithm iteratively explores the parameter space, using mutation operators to generate new solutions. The exploitation phase involves selecting the best solutions based on their fitness scores (i.e., the accuracy of the KELM model with the corresponding hyperparameter values).

The scouts search for the subsequent sleeping mound to make certain that the mongoose family does not return to the former one. Scout mobility relies on their ability to find a new sleeping mound. The following formula is used to simulate the movement of scout mongooses:

$$X_{i+1} = \begin{cases} X_i - CF \cdot \varphi \cdot \text{rand} \cdot (X_i - \vec{M}) & \text{if } \varphi_{i+1} > \varphi_i \\ X_i + CF \cdot \varphi \cdot \text{rand} \cdot (X_i - \vec{M}) & \text{else} \end{cases} \quad (13)$$

where rand is a random number between $[0,1]$, CF is the collective-volitive movement of the mongoose group controlling parameter, decreasing linearly with iterations and $\vec{M} = \sum_{i=1}^n X_i \cdot sm_i$ depicting the vector that dictates the mongoose's migration to the next sleeping mound.

3.5.3. Mutation Boosting

MB-DMOA incorporates mutation boosting, a feature that enhances the algorithm's ability to escape local optima. This process involves introducing diversity in the population by applying mutation operators, ensuring that the algorithm explores different regions of the parameter space. The polynomial mutation operator in MB-DMOA is utilized to improve the original DMOA's exploration and exploitation capabilities. This operator generates new solutions by applying a perturbation to the current solutions based on a polynomial distribution. The mutation operator is expressed as follows:

$$\delta = (2 \cdot \text{rand} - 1) \cdot \left(1 - (x/x_{\text{upper}})^{1/(1+\eta)}\right) \quad (14)$$

$$x' = x + \delta \cdot (x_{\text{upper}} - x_{\text{lower}}) \quad (15)$$

where δ is the polynomial mutation factor, rand is a random number between $[0,1]$, x is the current solution, x' is the new solution after mutation, x_{upper} and x_{lower} are the upper and lower bounds of the solution space and η is the distribution index, which controls the shape of the polynomial distribution.

3.5.4. Convergence

The phases of exploitation, mutation boosting, and exploration in the method are executed iteratively until a predetermined stopping criterion, such as completing a specified number of iterations, is satisfied. The solution with the highest fitness score is evaluated to identify the optimal set of hyperparameters for the KELM model. The algorithm iterates through these stages until the stopping criterion, which may be a predetermined goal fitness value or a maximum number of iterations, is met.

3.5.5. Optimal Solution

The optimal set of hyperparameters for the KELM model is determined by examining the solution with the highest fitness score.

Advantages of Using MB-DMOA in KELM Optimization

The MB-DMOA for KELM hyperparameter tuning offers several advantages:

- **Enhanced Exploration:** The mutation operators in the MB-DMOA method minimize the risk of the algorithm getting stuck in local optima by enabling the algorithm to explore a large region of the parameter space.
- **Efficient Exploitation:** The algorithm effectively exploits promising regions of the parameter space, converging towards the optimal solution.
- **Adaptability:** MB-DMOA is adaptable to different optimization problems, making it suitable for hyperparameter tuning in ML models like KELM.
- **Improved Performance:** By fine-tuning the hyperparameters of the KELM model, MB-DMOA ensures that the classifier performs optimally on the histopathological image classification task.

3.6. Fitness Function

In a proposed hybrid model, the fitness function plays a vital role in

guiding the MB-DMOA optimization algorithm toward optimal hyperparameters for the KELM classifier. In this case, the model proposes using classification accuracy as the fitness function for its simplicity and direct relation to the model's performance.

The fitness function $f(P)$ for the set of hyperparameters P is defined as the classification accuracy:

$$f(P) = \text{Accuracy}(P) \quad (16)$$

where P represent a specific set of hyperparameters for the KELM model, which includes kernel parameters and the regularization term, and $\text{Accuracy}(P)$ express the accuracy in classifying a validation dataset by the KELM model when trained with a particular hyperparameter P .

By experimenting with different combinations of hyperparameter P the MB-DMOA optimization method seeks to maximize this fitness function. For the KELM model, the optimal hyperparameter set is determined by selecting the configuration that produces the highest classification accuracy or fitness score.

The assessment of the model's performance in this situation relies on classification accuracy, a straightforward and practical metric. It expresses the percentage of accurately predicted instances in the validation dataset relative to the total instances. By maximizing classification accuracy, we aim to enhance the predictive capability of the KELM classifier in distinguishing cancerous and non-cancerous tissues.

4. Result and discussion

To assess the performance of both the proposed hybrid model and the MB-DMOA optimization algorithm, a series of experiments was conducted using the LC25000 datasets and GlaS datasets.

4.1. Experimental setup

The experiments were executed on a high-performance computing system, specifically an Intel Xeon E5-2697 v3 with a clock speed of 2.6 GHz, featuring 14 cores and 12 GB RAM. Additionally, a GPU in the form of an NVIDIA Tesla P100 with 16 GB memory was utilized in the computational setup.

The software environment was set up with the following tools: Python 3.7 as the programming language, TensorFlow 2.3 and Keras 2.4 as the DL framework, and Windows 10 as the Operating System.

4.2. Parameter setting

Table 1 contains the parameters utilized in the proposed model.

4.3. Evaluation Metrics

The metrics applied to measure the performance of the suggested hybrid strategy incorporate below metrics.

Accuracy: Accuracy is the fundamental evaluation metric that analyses the classifier's efficiency. The accuracy is calculated by employing equation (17).

Table 1

Hyperparameter with values.

Approaches	Hyperparameter	Value
MB-DMOA	Number of epochs	50
	Batch size	32
	Learning rate	0.001
	Mutation Probability	0.3
	Population Size	100
	Crossover Probability	0.7
	Maximum Iterations	50
KELM	Mutation Step Size (for KELM)	0.1
	Mutation Range (for KELM)	[0.1, 10]
	Mutation Probability (for KELM)	0.5

$$\text{Accuracy} = \frac{Z_{TN} + Z_{TP}}{Z_{FP} + Z_{TP} + Z_{FN} + Z_{TN}} \quad (17)$$

where Z_{FP} is the false positive, Z_{TP} denotes the true positive, Z_{FN} is the false negative, and Z_{TN} is the true negative.

Precision: The proportion of correctly identified specimens to the total positive specimens. The precision of the model is calculated by utilizing equation (18).

$$\text{Precision} = \frac{Z_{TP}}{Z_{FP} + Z_{TP}} \quad (18)$$

Sensitivity: The division of real samples that are accurately identified as belonging to a particular class of contaminants is referred to as the recall rate. The sensitivity of the classifier is calculated by utilizing equation (19).

$$\text{Recall} = \frac{Z_{TP}}{Z_{FN} + Z_{TP}} \quad (19)$$

Specificity: The ratio of true negatives to the sum of true negatives and false positives is known as model specificity. This metric signifies the proportion of false positives within the model. The below equation (20) describes the specificity of the approach.

$$\text{Specificity} = \frac{Z_{TN}}{Z_{TN} + Z_{FP}} \quad (20)$$

F1-Score: The harmonic mean of recall and precision provides a fair comparison of these two metrics. The below equation (21) is employed for calculating the F1-score of the proposed model.

$$\text{F1-score} = \frac{2 \times \text{recall} \times \text{precision}}{\text{precision} + \text{recall}} \quad (21)$$

4.4. Performance analysis

This part included illustrations of the confusion matrix, training, testing and validation accuracy, performance analysis, and LC25000 and Glas datasets.

The LC25000 dataset's confusion matrix is displayed in Fig. 2(a). It comprises five different classes that are used for dividing LC cancer based on both expected and actual classes. The LC25000 dataset contains twenty-five thousand photos in total. Fig. 2(b) illustrates the confusion matrix for the GlaS dataset, comprising two distinct classes. This confusion matrix comprises two categories such as healthy (benign tissue) and cancerous (malignant tissue) utilized to explain the interpretation of the classification model.

The simulation study generated Area Under the ROC (AUROC) plots for the proposed model, as depicted in Fig. 3(a), using both the LC25000 and GlaS datasets. An analysis of these AUROC values reveals that the proposed practice accomplished the highest scores, with 0.99 for

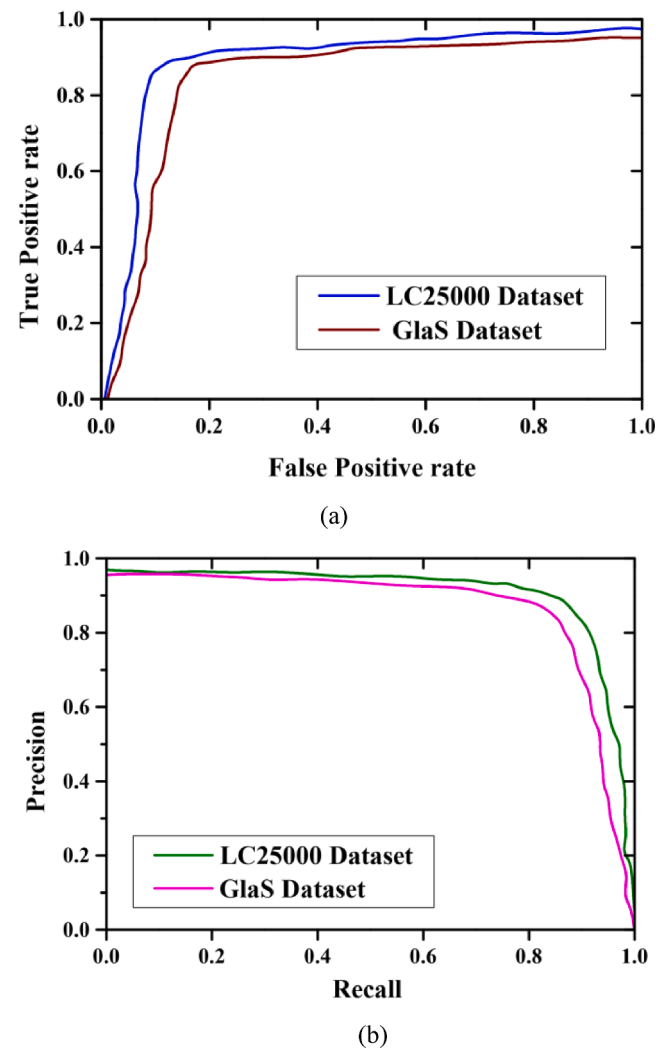


Fig. 3. Performance review of (a) AUROC and (b) AUPR.

LC25000 and 0.985 for GlaS. Fig. 3(b) displays the Area Under Precision-Recall (AUPR) values obtained for the proposed model, covering both the LC25000 and GlaS datasets. Upon examination, it becomes evident that the proposed strategy obtains the highest scores, with 0.994 for LC25000 and 0.987 for GlaS.

In Fig. 4(a), the depicted graph showcases the testing, training, and validation accuracy of the proposed strategy when applied to the

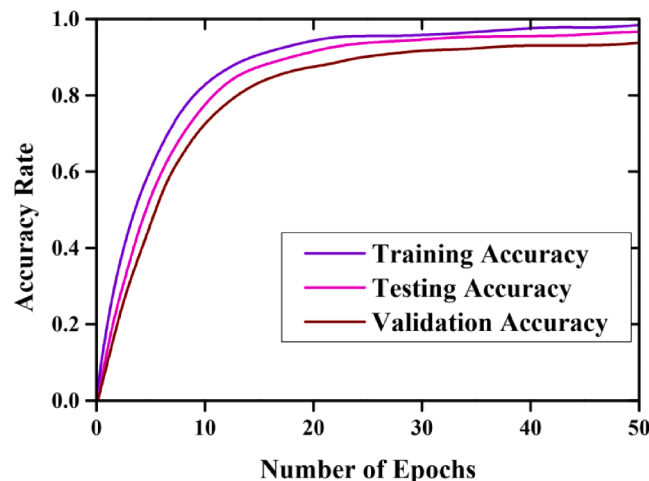
		Actual class				
		colon_aca	colon_n	lung_aca	lung_n	lung_sec
Predicted class	colon_aca	95	2	0	3	0
	colon_n	0	99	0	1	0
	lung_aca	0	2	91	5	2
	lung_n	1	0	2	97	0
	lung_sec	3	2	4	1	90

(a)

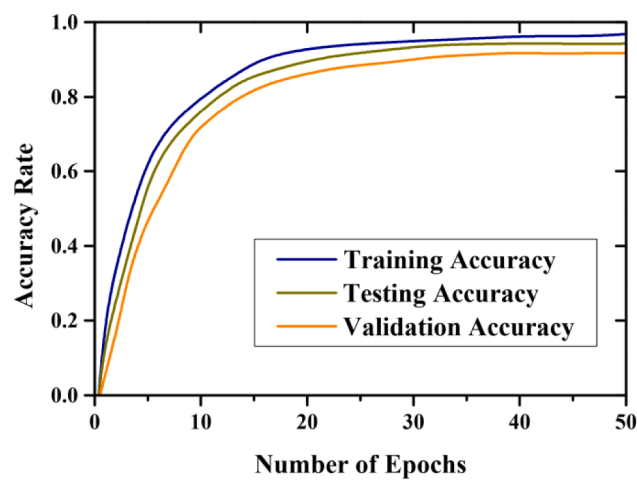
		Actual class	
		Benign	Malignant
Predicted class	Benign	98.9	1.1
	Malignant	5	95

(b)

Fig. 2. Confusion matrix for (a) LC25000 dataset and (b) GlaS dataset.



(a)



(b)

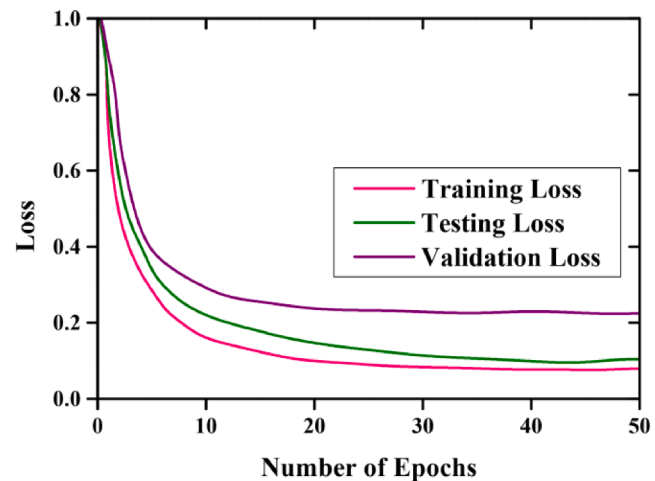
Fig. 4. Accuracy of training, testing, and validation using (a) LC25000 dataset and (b) GlaS dataset.

LC25000 dataset. The examination reveals notable performance, with the model achieving 0.991 in training, 0.968 in testing, and 0.932 in validation. Moving to Fig. 4(b), the displayed data presents the validation, testing, and training accuracy of the proposed practice on the GlaS dataset. An assessment of the outcomes highlights the model's consistent superiority, recording 0.989 in training, 0.955 in testing, and 0.921 in validation.

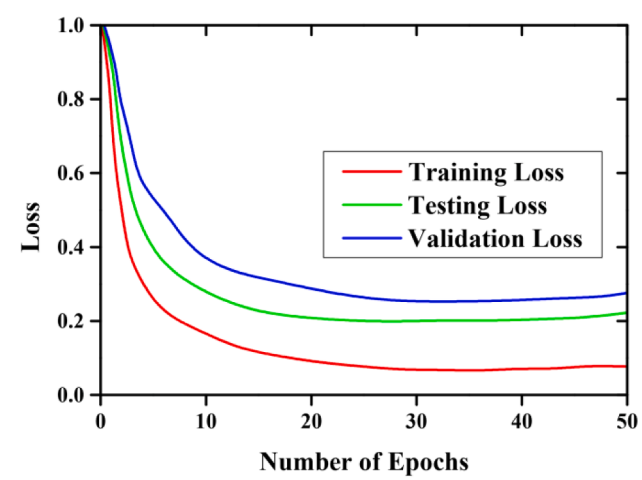
In Fig. 5(a), the chart depicts the training, testing, and validation loss values acquired by the proposed research, specifically on the LC25000 dataset. A scrutiny of the results indicates that the proposed strategy achieves comparatively minimal scores, recording 0.09 for training, 0.16 for testing, and 0.22 for validation. The representation in Fig. 5(b) highlights the training, testing, and validation loss values acquired for the proposed model, with a specific emphasis on the GlaS dataset. An examination of the data indicates that the proposed model consistently achieves low scores, with 0.11 for training, 0.21 for testing, and 0.29 for validation.

Table 2 showcases the performance analysis of various metrics based on the LC25000 and GlaS datasets.

Cross-validation: To ensure a diverse representation of samples in each set, the dataset was shuffled before splitting into training, validation, and test sets. To further assess the model's performance and reduce the impact of data splitting, a k-fold cross-validation strategy was employed. The dataset was divided into k folds, and the model was



(a)



(b)

Fig. 5. Training, testing, and validation loss of the (a) LC25000 dataset and (b) GlaS dataset.

Table 2
Analysis of different metric performance.

Metrics	LC25000 dataset	GlaS dataset
Accuracy(%)	99.0	98.9
Precision(%)	97.7	95.3
Sensitivity(%)	96.5	94.5
Specificity(%)	96.7	95.9
F1 score(%)	98.2	97.3

trained and evaluated k times, with a different fold for validation in each iteration. The cross-validation performance of the proposed study is illustrated in Table 3.

Table 3
Cross-validation Accuracy before stratified sampling.

Fold	LC25000 dataset	GlaS dataset
1	0.836	0.827
2	0.913	0.901
3	0.851	0.848
4	0.892	0.891
5	0.988	0.986
Mean	0.896	0.890
Standard deviation	0.053	0.054

The variation in the cross-validation performance is due to the presence of data imbalance within the dataset, influencing the performance of the model during cross-validation. To tackle this difficulty, a stratified sampling technique is implemented; this ensures that each fold of the cross-validation dataset maintains a balanced representation of samples across different classes. This approach mitigates the impact of data imbalance and provides a more equitable distribution of samples for training and evaluation.

After incorporating stratified sampling into the proposed methodology, the cross-validation experiment was conducted again and observed significantly improved consistency in performance across folds. The new cross-validation results demonstrate a reduction in variability and provide more reliable estimates of the model's performance. This enhancement strengthens the validity and robustness of the proposed strategy.

Stratified sampling: Stratified sampling is an approach in which the population is broken down into subgroups or strata according to specific characteristics. Then, samples are drawn at random from each stratum based on the proportion of the population it represents. By ensuring that every subgroup is fairly represented in the sample, this technique makes it possible to estimate population parameters with greater accuracy and dependability. When there is a lot of variability or heterogeneity in the population, stratified sampling is very helpful since it facilitates capturing the wide range of characteristics within the population. The cross-validation accuracy obtained after the stratified sampling is presented in [Table 4](#).

The LC classification outcomes with preprocessed and augmented outcomes of the proposed methodology using the LC25000 dataset and GlaS dataset are presented in [Table 5](#). The figures in the table prove that the proposed approach successfully classified various diseases such as lung_scc, lung_n, lung_aca, colon_n, and colon_aca, from the LC25000 dataset as well as benign and malignant classes from the Glas dataset.

The ablation study is presented in [Table 6](#). To ensure which technique is efficient for LC classification, the ablation study is performed. This demonstrates that the proposed practice with MB-DMOA attains high performance.

4.5. Comparative analysis

To provide a comprehensive comparison, let's discuss specific traditional ML methods and individual DL models used for comparison:

- **Support vector machine (SVM)** ([Lee et al., 2022](#)): In the context of histopathological image classification, SVM is used with handcrafted features extracted from the images.
- **RF** ([Gao et al., 2022](#)): In ensemble learning, Random Forest (RF) constructs a diverse array of decision trees during training, culminating in the classification decision being the mode among the classes predicted by these individual trees.
- **ResNet-50** ([Bukhari et al., 2020](#)): ResNet-50, widely applied in image classification, has demonstrated cutting-edge performance across diverse benchmarks.
- **DenseNet-121** ([Kumar et al., 2022](#)): In DenseNet, the connectivity pattern leads to more accurate gradients during backpropagation and helps in alleviating the vanishing gradient problem.

Table 4
Cross-validation Accuracy after stratified sampling.

Fold	LC25000 dataset	GlaS dataset
1	0.988	0.987
2	0.989	0.988
3	0.990	0.989
4	0.992	0.990
5	0.993	0.992
Mean	0.990	0.989
Standard deviation	0.0018	0.0015

- **InceptionV3** ([Garg and Garg, 2020](#)): InceptionV3 is another deep CNN that introduces the concept of inception modules, where filters of different sizes are applied to the input simultaneously, and their results are concatenated to produce the output. It is known for its efficiency in terms of computational cost and parameter count.
- **Lightweight DL Models and Transformation Methods (LDLT)** ([Attallah et al., 2022](#)): This model combines ShuffleNet, MobileNet, and SqueezeNet for the diagnosis of LC cancer. They demonstrate that they provide an improved explanation of the data, which improves the diagnosing procedure.
- **Global Context Attention Based CNN (GCA-CNN)** ([Provath et al., 2023](#)): The information about the spatial and the channel attention is captured using this model. From the input image, the extraction of semantic information is done.
- **ColonNet** ([Iqbal et al., 2023](#)): This model is the integration of global-local pyramid pattern (GLPP) and depth-wise separable convolutions. The mitotic patches are identified and classified using this approach.
- **DenseNet-ML models** ([Talukder et al., 2022](#)): This model integrates DenseNet with ML methods such as SVM, RF, etc. The feature extraction and detection are performed using the DenseNet and ML models. This reduces the cost and time.
- **InceptionV3-XGBoost-binary particle swarm optimization (BPSO)** ([Deif et al., 2022](#)): Extraction of feature is performed using the pre-trained model, best features are selected using the BPSO and the classification of cancer is performed using the XGBoost. This provides accurate prediction.
- **VGG-ResNet50** ([Yildiz and Yakut, 2023](#)): This model provides a diagnosis of colon cancer with superior accuracy. This is also utilized in the decision-making system.

[Table 7](#) illustrates the performance of different algorithms. The findings suggest that the proposed model excels in accuracy, sensitivity, precision, F1 score, and specificity compared to other algorithms.

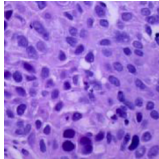
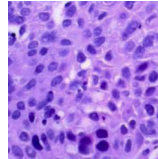
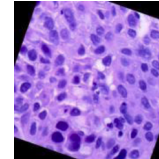
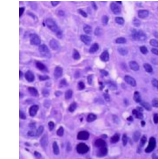
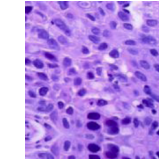
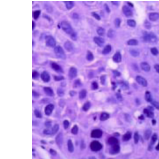
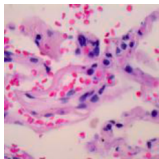
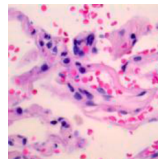
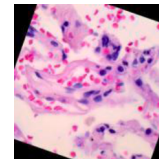
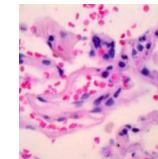
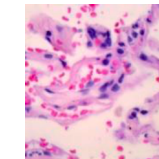
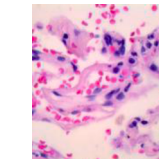
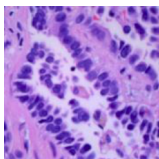
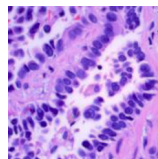
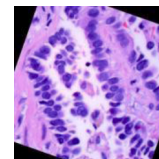
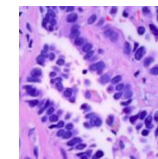
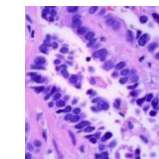
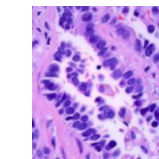
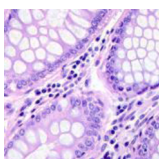
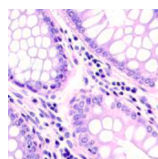
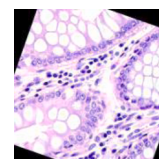
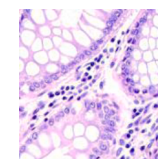
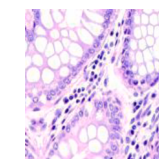
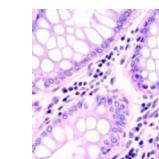
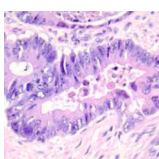
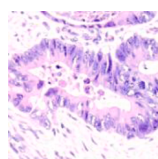
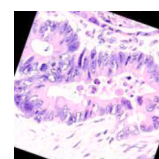
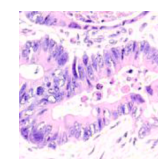
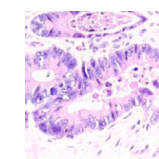
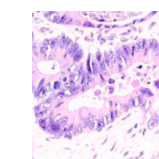
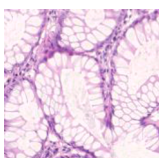
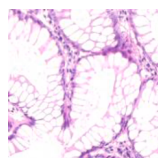
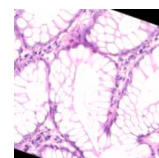
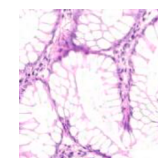
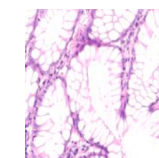
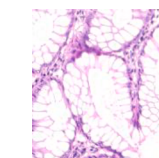
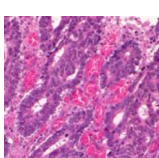
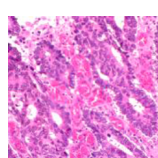
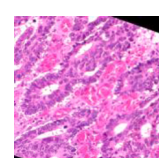
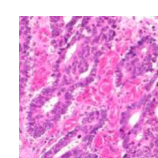
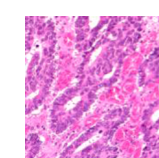
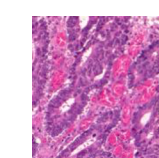
Within the framework of this study, the suggested hybrid model's performance was examined and compared with that of individual DL models and traditional methods. Metrics including accuracy, specificity, F1-score, sensitivity, precision, and specificity were used in this comparison. The outcomes demonstrated the hybrid model's higher performance and demonstrated how well it combined previously trained DL models along with KELM for the recognition of LC cancer using histopathology images.

4.6. Discussion

Cancer is the main reason for death worldwide. Detecting the cancer in the early stage aids in treating it. Several techniques have been developed for LC cancer classification but they suffer from high processing time and inaccurate classification. The proposed strategy overcomes these challenges. The preprocessing step involves normalizing the pixel values, resizing the images, and splitting the images. Data augmentation techniques such as random rotation, flipping, elastic deformation, and zoom factor are applied to enhance the performance ability of the approach. In the ResNet50 model, a set of residual functions is learned using the residual connections, that map the input to the appropriate output. CNN architecture from the inception family is InceptionV3, which is utilized to propagate label information and label smoothing. Only less computational resources are required for fine-tuning the inception model. The interdependence between the layers is mitigated by the reuse of the feature map in the DenseNet model. This also reduces the gradient disappearance problem. By integrating the advantages of three pre-trained models, the proposed model is enhanced, and complex patterns are identified. A variant of ELM is known as KELM. Benefits of the basic ELM include quick learning and excellent generalization ability. The KELM inherits the advantage of ELM with stable and superior performance. Using this KELM, the

Table 5

A visual depiction of images for LC classification within the LC25000 and GlaS datasets. This offers a thorough visualization of the dataset, elucidating its associated outcomes.

LC25000 dataset						
Input image	Augmented image				Classification image	Class name
	Flipping	Random rotation	Zoom factor	Elastic deformation		
						lung_scc
						lung_n
						lung_aca
						colon_n
						colon_aca
GlaS dataset						
						benign
						malignant

intricate image features are handled and high dimensional data is efficiently classified. In the proposed approach, we combined mutation operation with DMO. The mutation operation mitigates the local optima problem. The phases of exploitation, mutation boosting, and exploration in the method are executed iteratively until a predetermined stopping criterion, such as completing a specified number of iterations, is satisfied. The solution with the highest fitness score is evaluated to identify the optimal set of hyperparameters for the KELM model. The mutation-boosted DMO provides improved exploration and effective exploitation.

By fine-tuning the hyperparameters of the KELM model, MB-DMOA achieves optimal performance on the histopathological image classification task. Overall the combination of pre-trained models (ResNet50, InceptionV3, and DenseNet), KELM, and MB-DMOA provides more efficient classification.

4.6.1. Impact of Parameter Optimization using MB-DMOA

The application of MB-DMOA to fine-tune hyperparameters significantly impacted the hybrid model's performance. By optimizing KELM's

Table 6
Results of the ablation study.

Metrics	Proposed approach	
	Without optimization	With MB-DMOA
Accuracy(%)	91.7	98.9
Precision(%)	89.9	96.7
Sensitivity(%)	87.5	95.8
Specificity(%)	86.3	96.5
F1 score(%)	90.2	97.6

hyperparameters, MB-DMOA ensured the classifier's optimal functionality in the diagnostic task. Table 5 displays the ablation study.

The hybrid model performed better than its non-optimized counterpart on several measures after undergoing MB-DMOA-based optimization, according to the results. This highlights the importance of parameter tuning in maximizing the model's predictive capabilities.

4.6.2. Interpretation of Results and Implications for Cancer Diagnosis

The results of the studies conducted highlight the efficacy of the hybrid model in diagnosing LC cancer based on histopathological images. The improved precision and recall of the model, along with its balanced precision and recall, showcase its ability to accurately identify malignant tissues while effectively minimizing the number of false positives and false negatives.

The noticeable superiority demonstrated by the hybrid model, surpassing both individual DL models and conventional methods, highlights the vital significance of integrating the advantages of KELM with pre-trained DL models to achieve accurate cancer diagnosis. The rich feature representation and robust classification capabilities contribute to the model's diagnostic accuracy.

Furthermore, the impact of parameter optimization using MB-DMOA highlights the significance of tuning hyperparameters to achieve optimal performance. The optimization process ensures that the model is fine-tuned to the specific diagnostic task, leading to improved classification results.

The implications of these results for cancer diagnosis are substantial. Utilizing the hybrid model, pathologists and oncologists can diagnose and categorize LC cancer. This model facilitates early cancer detection, leading to timely interventions and improved patient outcomes, providing accurate and reliable classifications.

5. Conclusion and Future Scope

This study presents a hybrid approach for the diagnosis of LC cancer from histopathology images. Resizing histopathological images to 224x224, normalizing pixel values to [-1, 1] through mean subtraction and standard deviation scaling. The dataset is divided into training (70 %), validation (20 %), and testing (10 %) sets, with label encoding used during training. The augmentation is applied to improve the model's

generalization and to prevent overfitting. The hybrid model leverages the learned features of pre-trained DL models (ResNet-50, InceptionV3, DenseNet) for extracting features from histopathological images. Feature fusion combines ResNet-50, InceptionV3, and DenseNet features into a single comprehensive vector, enhancing the model's ability to recognize intricate patterns indicative of malignant tissues. The final model component, KELM, efficiently classifies high-dimensional data, crucial for managing complex image attributes. To prevent overfitting, regularization techniques are integrated into the training process of the KELM classifier, along with the DL models, for optimal tuning. Optimization involves enhancing exploration and exploitation using MB-DMOA parameter tuning for KELM. In histopathological image categorization, MB-DMOA improves KELM performance, providing better exploration, efficient exploitation, and flexibility. This model combines the robust classification capabilities of KELM with the feature extraction expertise of pre-trained DL models. The integration of features extracted from ResNet-50, InceptionV3, and DenseNet with KELM provided a rich representation of the histopathological images, resulting in more accurate classifications. Achieving an accuracy (98.9 %), sensitivity (95.8 %), precision (96.7 %), F1-score (97.6 %), and specificity (96.5 %), the model exhibited commendable performance. The proposed hybrid model showcased its effectiveness in cancer diagnosis, outperforming both individual DL models and traditional ML techniques. Incorporating MB-DMOA for hyperparameter adjustment significantly enhanced the model's performance. The optimization process ensured the model was fine-tuned for the specific diagnostic task, resulting in improved classification outcomes. The success of MB-DMOA in tuning the hyperparameters of KELM demonstrated the algorithm's adaptability and effectiveness in parameter optimization for ML models. While the research demonstrates the potential of the hybrid model in cancer diagnosis from histopathological images, there are several avenues for future work: Larger and more diverse datasets, obtained through multi-center studies, can serve to further validate the robustness and generalizability of the proposed hybrid model. Clinical data, including medical history and patient demographics, can be added to the algorithm to improve its predicted accuracy and give oncologists a more thorough evaluation.

Ethical Statements:

Funding

Not applicable.

Compliance with Ethical Standards.

Human and Animal Rights.

This article does not contain any studies with human or animal subjects performed by any of the authors.

Informed Consent.

Informed consent was obtained from all individual participants included in the study.

Consent to participate: Not applicable.

Consent for publication: Not applicable.

Availability of data and material:

Table 7
Comparative examination of different techniques.

Methods	Accuracy (%)	Precision (%)	Sensitivity (%)	Specificity (%)	F1 score (%)	Execution time(s)
SVM	88.3	86.3	79.3	78.2	86.3	4.2
RF	85.2	82.3	81.2	75.4	80.2	4.3
ResNet-50	83.9	82.0	78.5	75.2	74.6	3.9
Inception V3	87.7	95.5	94.1	91.8	93.8	5.3
DenseNet 121	89.5	91.2	88.2	89.1	91.9	4.2
LDLT	96.3	94.3	90.3	92.2	96.3	4.7
GCA-CNN	93.3	87.3	90.2	91.4	88.2	6.1
ColonNet	94.3	85.3	91.2	93.4	85.2	5.6
DenseNet-ML	95.3	91.4	89.5	91.4	89.9	5.2
InceptionV3-XGBoost-BPSO	96.6	92.4	91.0	94.4	95.1	7.3
VGG-ResNet50	96.0	93.9	86.7	93.3	92.7	6.2
Proposed	98.9	96.7	95.8	96.5	97.6	3.1

The data that support the findings of this study are available from the corresponding author upon reasonable request.

Declaration of competing interest

The authors declare that they have no known competing financial interests or personal relationships that could have appeared to influence the work reported in this paper.

Data availability

Data will be made available on request.

Acknowledgements

Not applicable

References

- Agushaka, J. O., Ezugwu, A. E., & Abualigah, L. (2022). Dwarf mongoose optimization algorithm. *Computer methods in applied mechanics and engineering*, 391, Article 114570.
- Akinola, O. A., Agushaka, J. O., & Ezugwu, A. E. (2022). Binary dwarf mongoose optimizer for solving high-dimensional feature selection problems. *Plos one*, 17(10), e0274850.
- Alboaneen, D., Alqarni, R., Alqahtani, S., Alrashidi, M., Alhuda, R., Alyahyan, E., & Alshammari, T. (2023). Predicting Colorectal Cancer Using Machine and Deep Learning Algorithms: Challenges and Opportunities. *Big Data and Cognitive Computing*, 7(2), 74.
- Attallah, O., Aslan, M. F., & Sabancı, K. (2022). A framework for lung and colon cancer diagnosis via lightweight deep learning models and transformation methods. *Diagnostics*, 12(12), 2926.
- Baranwal, N., Doravari, P., & Kachhoria, R. (2021). Classification of histopathology images of lung cancer using convolutional neural network (CNN). *Disruptive Developments in Biomedical Applications*, (p.75).
- Borkowski, A.A., Bui, M.M., Thomas, L.B., Wilson, C.P., Del, L.A., & Mastorides, S.M. (2019). Lung and colon cancer histopathological image dataset (lc25000). *arXiv preprint arXiv:1912.12142*.
- Bukhari, S.U.K., Asmara, S., Bokhari, S.K.A., Hussain, S.S., Armaghani, S.U., & Shah, S.S. H. (2020). The Histological Diagnosis of Colonic Adenocarcinoma by Applying Partial Self-Supervised Learning. *medRxiv*.
- Deif, M.A., Attar, H., Amer, A., Elhaty, I.A., Khosravi, M.R., & Solyman, A.A. (2022). Diagnosis of oral squamous cell carcinoma using deep neural networks and binary Particle Swarm optimization on histopathological images: an AloMT approach. *Computational Intelligence and Neuroscience*, 2022.
- Elnakib, A., Amer, H. M., & Abou-Chadi, F. E. (2020). Early lung cancer detection using deep learning optimization. *International Journal of Online and Biomedical Engineering (IJOE)*, 16(06), 82–94.
- Gao, Y., Zhu, Z., & Sun, F. (2022). Increasing prediction performance of colorectal cancer disease status using random forests classification based on metagenomic shotgun sequencing data. *Synthetic and systems biotechnology*, 7(1), 574–585.
- Garg, S., & Garg, S. (2020, December). Prediction of lung and colon cancer through analysis of histopathological images by utilizing Pre-trained CNN models with visualization of class activation and saliency maps. In *Proceedings of the 2020 3rd Artificial Intelligence and Cloud Computing Conference* (pp. 38–45).
- Hadiyoso, S., Aulia, S., & Irawati, I. D. (2023). Diagnosis of lung and colon cancer based on clinical pathology images using convolutional neural network and CLAHE framework. *International Journal of Applied Science and Engineering*, 20(1), 1–7.
- Hasan, M.I., Ali, M.S., Rahman, M.H., & Islam, M.K., (2022). Automated detection and characterization of colon Cancer with deep convolutional neural networks. *Journal of Healthcare Engineering*, 2022.
- Hatuwal, B. K., & Thapa, H. C. (2020). Lung cancer detection using convolutional neural network on histopathological images. *Int. J. Comput. Trends Technol.*, 68(10), 21–24.
- Ho, C., Zhao, Z., Chen, X. F., Sauer, J., Saraf, S. A., Jialdasani, R., Taghipour, K., Sathe, A., Khor, L. Y., Lim, K. H., & Leow, W. Q. (2022). A promising deep learning-assistive algorithm for histopathological screening of colorectal cancer. *Scientific Reports*, 12(1), 2222.
- Iqbal, S., Qureshi, A. N., Alhussein, M., Aurangzeb, K., & Kadry, S. (2023). A Novel Heteromorphous Convolutional Neural Network for Automated Assessment of Tumors in Colon and Lung Histopathology Images. *Biomimetics*, 8(4), 370.
- Jiao, Y., Li, J., Qian, C., & Fei, S. (2021). Deep learning-based tumor microenvironment analysis in colon adenocarcinoma histopathological whole-slide images. *Computer Methods and Programs in Biomedicine*, 204, Article 106047.
- Kumar, N., Sharma, M., Singh, V. P., Madan, C., & Mehandia, S. (2022). An empirical study of handcrafted and dense feature extraction techniques for lung and colon cancer classification from histopathological images. *Biomedical Signal Processing and Control*, 75, Article 103596.
- Lai, Y. H., Chen, W. N., Hsu, T. C., Lin, C., Tsao, Y., & Wu, S. (2020). Overall survival prediction of non-small cell lung cancer by integrating microarray and clinical data with deep learning. *Scientific reports*, 10(1), 4679.
- Lee, J. E., Do, L. N., Jeong, W. G., Lee, H. J., Chae, K. J., Kim, Y. H., & Park, I. (2022). A Radiomics Approach on Chest CT Distinguishes Primary Lung Cancer from Solitary Lung Metastasis in Colorectal Cancer Patients. *Journal of Personalized Medicine*, 12(11), 1859.
- Lee, S. H., Song, I. H., & Jang, H. J. (2021). Feasibility of deep learning-based fully automated classification of microsatellite instability in tissue slides of colorectal cancer. *International Journal of Cancer*, 149(3), 728–740.
- Li, M., Ma, X., Chen, C., Yuan, Y., Zhang, S., Yan, Z., Chen, C., Chen, F., Bai, Y., Zhou, P., & Lv, X. (2021). Research on the auxiliary classification and diagnosis of lung cancer subtypes based on histopathological images. *Ieee Access*, 9, 53687–53707.
- Mangal, S., Chaurasia, A., & Khajanchi, A. (2020). Convolution neural networks for diagnosing colon and lung cancer histopathological images. *arXiv preprint arXiv: 2009.03878*.
- Naseer, I., Akram, S., Masood, T., Jaffar, A., Khan, M. A., & Mosavi, A. (2022). Performance analysis of state-of-the-art CNN architectures for luna16. *Sensors*, 22(12), 4426.
- Obayya, M., Arasi, M. A., Alruwaisi, N., Alsini, R., Mohamed, A., & Yaseen, I. (2023). Biomedical Image Analysis for Colon and Lung Cancer Detection using Tuna Swarm Algorithm with Deep Learning Model. *IEEE Access*, 11, 94705–94712.
- Provath, M. A. M., Deb, K., Dhar, P. K., & Shimamura, T. (2023). *Classification of Lung and Colon Cancer Histopathological Images Using Global Context Attention Based Convolutional Neural Network*. IEEE Access.
- Raihan, M. J., & Nahid, A. A. (2023). Classification of histopathological colon cancer images using particle swarm optimization-based feature selection algorithm. In *Diagnostic Biomedical Signal and Image Processing Applications with Deep Learning Methods* (pp. 61–82). Academic Press.
- Rajesh, M. N., & Chandrasekar, B. S. (2023). Multi-Class Classification Of Pca Mr Images Based On Ucla Score Using Deep Learning Resnet-50 Model. *Journal of Biomechanical Science and Engineering*.
- Rajesh, P., Murugan, A., Murugamantham, B., & Ganesh, S. (2020). Lung cancer diagnosis and treatment using AI and Mobile applications. *International Journal of Interactive Mobile Technologies (ijIMT)*, 14(17), 189–203.
- Sakr, A. S., Soliman, N. F., Al-Gaashani, M. S., Plawiak, P., Ateya, A. A., & Hammad, M. (2022). An efficient deep learning approach for colon cancer detection. *Applied Sciences*, 12(17), 8450.
- Salimi, S., Lanjanian, H., Abbasi, K., Salimi, M., Najafi, A., Tapak, L., & Masoudi-Nejad, A. (2023). A deep learning-based framework for predicting survival-associated groups in colon cancer by integrating multi-omics and clinical data. *Heliyon*, 9(7).
- Talukder, M. A., Islam, M. M., Uddin, M. A., Akhter, A., Hasan, K. F., & Moni, M. A. (2022). Machine learning-based lung and colon cancer detection using deep feature extraction and ensemble learning. *Expert Systems with Applications*, 205, Article 117695.
- Tasnim, Z., Chakraborty, S., Shamrat, F. J. M., Chowdhury, A. N., Nuha, H. A., Karim, A., Zahir, S. B., & Billah, M. M. (2021). Deep learning predictive model for colon cancer patients using CNN-based classification. *International Journal of Advanced Computer Science and Applications*, 12(8), 687–696.
- Tummala, S., Kadry, S., Nadeem, A., Rauf, H. T., & Gul, N. (2023). An Explainable Classification Method Based on Complex Scaling in Histopathology Images for Lung and Colon Cancer. *Diagnostics*, 13(9), 1594.
- yahia Ibrahim, N., & Talaat, A. S. (2022). An Enhancement Technique to Diagnose Colon and Lung Cancer by Using Double CLAHE and Deep Learning. *International Journal of Advanced Computer Science and Applications*, 13(8).
- Ye, A.Z., Li, B.R., Zhou, C.W., Wang, D.M., Mei, E.M., Shu, F.Z., & Shen, G.J. (2023). High-Dimensional Feature Selection Based on Improved Binary Ant Colony Optimization Combined with Hybrid Rice Optimization Algorithm. *International Journal of Intelligent Systems* 2023. (27).
- Yıldız, G., & Yakut, Ö. (2023). Diagnostic Decision Making on Medical Images Using Deep Learning Models. *Eurasia Journal of Mathematics, Engineering, Natural & Medical Sciences*, 10(28), 130–142.
- Yu, G., Sun, K., Xu, C., Shi, X. H., Wu, C., Xie, T., Meng, R. Q., Meng, X. H., Wang, K. S., Xiao, H. M., & Deng, H. W. (2021). Accurate recognition of colorectal cancer with semi-supervised deep learning on pathological images. *Nature communications*, 12(1), 6311.
- Zhang, M., Li, W., Zhang, L., Jin, H., Mu, Y., & Wang, L. (2023). A Pearson correlation-based adaptive variable grouping method for large-scale multi-objective optimization. *Information Sciences*, 639, Article 118737.
- Zhang, Y., Wu, C., Tian, Y., & Zhang, X. (2024). A co-evolutionary algorithm based on sparsity clustering for sparse large-scale multi-objective optimization. *Engineering Applications of Artificial Intelligence*, 133, Article 108194.
- Zhou, C., Jin, Y., Chen, Y., Huang, S., Huang, R., Wang, Y., Zhao, Y., Chen, Y., Guo, L., & Liao, J. (2021). Histopathology classification and localization of colorectal cancer using global labels by weakly supervised deep learning. *Computerized Medical Imaging and Graphics*, 88, Article 101861.